Article

Constraining the trend in the ocean CO$_2$ sink during 2000–2022

Nicolas Mayot [1] ✉, Erik T. Buitenhuis[1], Rebecca M. Wright [1], Judith Hauck [2,3], Dorothee C. E. Bakker [1] & Corinne Le Quéré [1]

The ocean will ultimately store most of the CO$_2$ emitted to the atmosphere by human activities. Despite its importance, estimates of the 2000–2022 trend in the ocean CO$_2$ sink differ by a factor of two between observation-based products and process-based models. Here we address this discrepancy using a hybrid approach that preserves the consistency of known processes but constrains the outcome using observations. We show that the hybrid approach reproduces the stagnation of the ocean CO$_2$ sink in the 1990s and its reinvigoration in the 2000s suggested by observation-based products and matches their amplitude. It suggests that process-based models underestimate the amplitude of the decadal variability in the ocean CO$_2$ sink, but that observation-based products on average overestimate the decadal trend in the 2010s. The hybrid approach constrains the 2000–2022 trend in the ocean CO$_2$ sink to 0.42 ± 0.06 Pg C yr^{-1} decade^{-1}, and by inference the total land CO$_2$ sink to 0.28 ± 0.13 Pg C yr^{-1} decade^{-1}.

The ocean plays a crucial role in the global carbon cycle and climate. Every year, it absorbs, on average, 25% of the anthropogenic CO$_2$ emitted to the atmosphere from burning fossil fuels and land-use change[1,2]. The ocean will be the main storage for most of the CO$_2$ emitted to the atmosphere from human activities, absorbing more than half of the cumulative emissions on a timescale of 1000 years, and between 60% and 85% on timescales of 10,000 years or longer[3]. The ocean CO$_2$ sink responds mainly to the increase in atmospheric CO$_2$ and is the result of processes taking place on different timescales: the dissolution of anthropogenic CO$_2$ at the surface, its buffering by carbonate chemistry, and its transport to the intermediate and deep ocean by ocean circulation[4]. This uptake is modulated by the variable growth rate in atmospheric CO$_2$[5]. Furthermore, the ocean carbon reservoir is also sensitive to climate variability and climate change[6,7], which modulates the response of the ocean CO$_2$ sink to anthropogenic CO$_2$ emissions, generates variability, and can alter both the decadal rate of change and long-term storage of carbon in the ocean. An accurate estimate of the trends and variability in the ocean CO$_2$ sink is needed to better understand how the ocean carbon cycle responds to the various drivers of change and to predict its evolution and its long-term fate. An accurate assessment of the ocean CO$_2$ sink and its

variability also provides an independent constraint on the other terms of the global carbon budget, in particular the trend and variability of the CO$_2$ sink by the terrestrial biosphere[8].

Over the last two decades, considerable progress has been made in improving our quantitative assessment of the ocean CO$_2$ sink and its trend and variability. The IPCC Fourth Assessment Report[9] assessed a mean ocean CO$_2$ sink for the 1990s based on observations of 2.2 ± 0.4 Pg C yr^{-1}, which has stood the test of time[1,3]. The first estimates of the ocean CO$_2$ sink were based on ocean general circulation models[10], followed by estimates inferred from O$_2$/N$_2$ observations[11,12] and broader geochemical data[10,13]. Later, the development of global ocean biogeochemical models (GOBMs) provided the first estimates of the ocean CO$_2$ sink variability in response to climate variations and long-term increases in atmospheric CO$_2$ concentration[14,15]. These models simulate the processes that regulate the full carbon cycle in the ocean (both natural and anthropogenic) and respond to changes in climate, weather, and variations in CO$_2$ levels in the atmosphere. Results from such process-based ocean models have suggested that the ocean CO$_2$ sink is sensitive to climate change and variability but that this variability is much smaller than the trend induced by the rising atmospheric CO$_2$[16].

[1]School of Environmental Sciences, University of East Anglia, Norwich, UK. [2]Alfred-Wegener-Institut, Helmholtz-Zentrum für Polar- und Meeresforschung, Bremerhaven, Germany. [3]Universität Bremen, Bremen, Germany. ✉e-mail: n.mayot@uea.ac.uk

More recently, observation-based estimates of the ocean CO_2 sink have become available from multiple data products. This has been made possible by the annual release of quality-controlled observations of CO_2 fugacity (fCO_2) at the sea surface—analogous to the partial pressure of CO_2—compiled within the Surface Ocean CO_2 Atlas (SOCAT) since 2015[17,18], and the emergence of machine learning and other advanced numerical approaches to extrapolate these relatively sparse space-time observations of fCO_2. Estimates from these observation-based products (fCO_2-products), which all used the SOCAT database as a starting point, confirmed some aspects of the ocean CO_2 sink simulated by the GOBMs, including the mean ocean CO_2 sink within observational uncertainties, the presence of a hiatus in its growth rate in the 1990s[19,20], and of variability much smaller than its long-term trend[2]. It should be noted that these fCO_2-products only assess the air-sea CO_2 flux, and not where anthropogenic CO_2 is ultimately stored in the ocean, which would require additional measurements of carbon in the water column, as well as more assumptions[21–24].

Despite recent progress, the two types of estimates used within the global carbon budget annual update by the carbon research community diverge over the last two decades (2000–2022)[22,23,25], with the fCO_2-product ensemble suggesting a decadal rate of growth of the ocean CO_2 sink almost twice as high as that simulated by the GOBMs ensemble (Table 1)[2,25]. The systematic nature of this discrepancy suggests a structural error in one or both methodologies used. In addition, the fCO_2-products suggest a higher amplitude of decadal variability on average than that simulated by the GOBMs over the period 1990–2022 (Table 1, Supplementary Fig. S1)[2]. Results from models using data assimilation[26,27] also suggest an underestimated decadal variability in GOBMs air-sea CO_2 flux[28,29]. This lack of consistency between the fCO_2-products and the GOBMs ensemble originates in the mid- and high-latitude regions of both hemispheres (poleward of 30°N and 30°S)[2].

We focus here on understanding the factor-of-two inconsistency in estimates of the 2000–2022 trend in the ocean CO_2 sink between fCO_2-products and GOBMs, which occurs despite the increasing number of fCO_2 observations (i.e., from ~4500 gridded observational data points a year in the 1990s, to 10,000 in the 2000s, and 15,000 in the 2010s). We introduce and use a hybrid approach that uses, as a starting point, the NEMO-PlankTOM12.1 GOBM forced with meteorological and climate reanalysis data from the National Centres for Environmental Prediction (NCEP[30]) and observed atmospheric CO_2 concentration. The hybrid approach then constrains the model outcome on a yearly basis using SOCAT observations to provide an annual estimate of the ocean CO_2 sink (see methods). NEMO-PlankTOM12.1 is the latest update of an established GOBM that was used from the onset in the annual updates of the global carbon budget analysis and which was designed for the study of the ocean CO_2 sink variability[31]. Its overall performance in simulating ocean physics and biogeochemistry is comparable to that of other GOBMs in the global carbon budget analysis (see methods, Table 1, Supplementary Figs. S2 and S3)[2,19].

The hybrid approach preserves the coherence of the physical and biogeochemical processes represented in NEMO-PlankTOM12.1 and goes beyond the traditional model evaluation by constraining the model output fields of fCO_2 against the observed fCO_2 data provided by SOCAT. A similar hybrid approach was recently published[32], but with a machine learning algorithm used to derive the factors influencing the fCO_2 variability. Here, the mechanism as represented in the NEMO-PlankTOM12.1 model, including the mixed-layer dynamics and the large-scale circulation, the carbonate chemistry, and the organic carbon transfer to depth resulting from biological processes (see methods for a description of the model) remained unchanged and thus also constrained the results. The hybrid approach used here thus provides an estimate of the ocean CO_2 sink that is based on both observations and on current theoretical understanding of the response of the ocean CO_2 sink to climate change and variability. Note that the hybrid approach used here, which optimises a target variable using multiple model simulations and a cost function, has been used in previous studies to constrain global ocean primary production[33] and air-sea fluxes of N_2O[34] and CCl_4[35].

Results

Constraints on the decadal variability of the global ocean CO_2 sink

In order to use observations to constrain the annual global ocean CO_2 sink simulated by NEMO-PlankTOM12.1 standard model simulation, perturbed simulations were deliberately produced. This was obtained by perturbing model parameters. Perturbed simulations provided a range of possible values for the ocean CO_2 sink around the estimate from the standard model simulation, and covered the expected range suggested by the global carbon budget analysis. We show here results obtained with the perturbation of the half-saturation constant of bacterial remineralization, which is more homogeneous and, therefore, more robust (see methods and the Supplementary information for details of the sensitivity analyses). Then, for each year, the optimal CO_2 sink was found within this range of possibilities by optimising the calculated mean square error (MSE) between the simulated fCO_2 and the SOCAT observations. The hybrid approach also provides a quantitative estimate of uncertainty (see methods).

The hybrid approach increases the decadal variability of the ocean CO_2 sink simulated by the NEMO-PlankTOM12.1 process-based ocean model (see methods for the definition of decadal variability). Originally, over the period 1990–2022, NEMO-PlankTOM12.1 simulated amplitudes of decadal variability for the ocean CO_2 sink of 0.11 Pg C yr^{-1}. This value is at the high end of the decadal variability simulated by the other GOBMs used in the global carbon budget analysis (Table 1). The hybrid approach further increases this simulated decadal variability by 18% to 0.13 ± 0.02 Pg C yr^{-1}, to a value close to the decadal variability estimated by the fCO_2-products (0.14 ± 0.06 Pg C yr^{-1}).

We tested the robustness of the decadal variability produced by the hybrid approach with respect to (i) the choice in the selected model's configuration and parameter perturbed, and (ii) the annual availability and distribution of the SOCAT data. To do this, we first

Table 1 | Temporal variability of the ocean CO_2 sink estimated using different methods

Methods	Amplitude of decadal variability (Pg C yr^{-1})	Decadal trends (Pg C yr^{-1} $decade^{-1}$)			
	1990–2022	1990s	2000s	2010s	2000–2022
Process-based models					
GCB's GOBMs	0.08 ± 0.02	0.11 ± 0.16	0.40 ± 0.10	0.34 ± 0.08	0.28 ± 0.05
NEMO-PlankTOM12.1	0.11	0.02	0.27	0.53	0.33
Observation-based products					
GCB's fCO_2-products	0.14 ± 0.06	-0.12 ± 0.35	0.71 ± 0.38	0.68 ± 0.19	0.54 ± 0.13
Hybrid approach					
This study	0.13 ± 0.02	-0.19 ± 0.17	0.80 ± 0.21	0.44 ± 0.15	0.42 ± 0.06
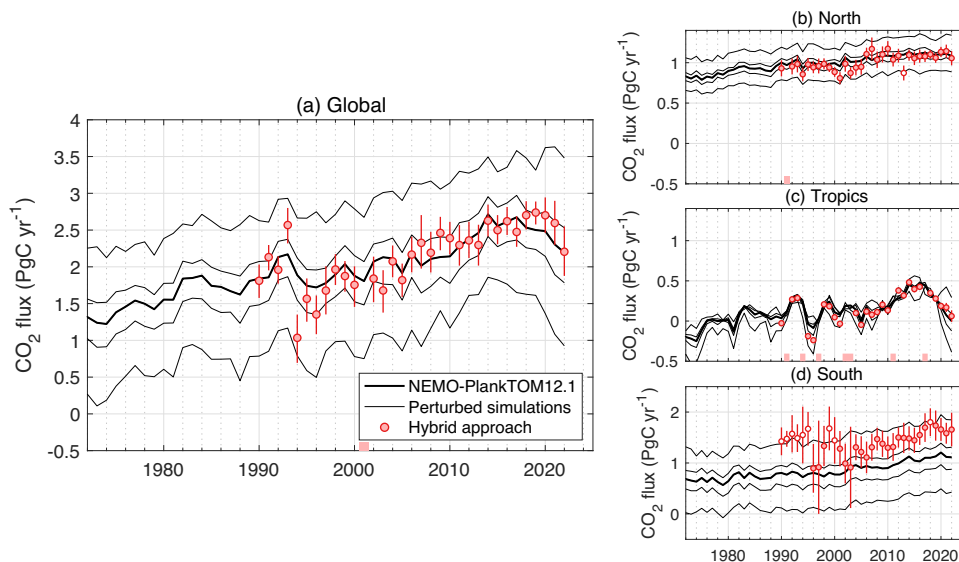
Fig. 1 | Ocean CO$_2$ sink constrained at global scale and by latitude bands between 1990 and 2022. Positive values denote a sink for CO$_2$. **a** The global ocean is divided into three latitudinal bands: **b** North (>30°N), **c** Tropics (30°N–30°S), and **d** South (<30°S). The thick black line represents NEMO-PlankTOM12.1 standard simulation, the thin black lines represent the perturbed simulations, and the red dots represent the estimate using the hybrid approach with ±1σ (68%) confidence
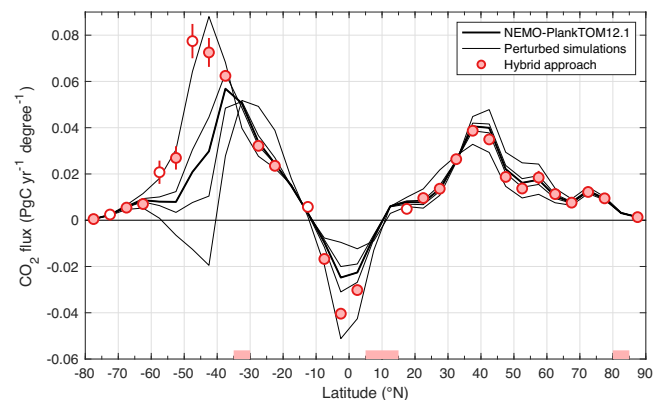
interval. On the *x* axis, the years highlighted in red have an unconstrained ocean CO$_2$ sink. Empty red dots are years with an ocean CO$_2$ sink value constrained but outside the bounds of the perturbation experiments (i.e., uncertain values, see methods). The perturbed simulations are produced by varying the half-saturation constant of bacterial remineralisation (from 5×10^{-6} mol L^{-1} to 18×10^{-6} mol L^{-1}).

applied the hybrid approach to a total of six different model setups (see methods). This first sensitivity analysis suggested a comparable increase in decadal variability (0.16 ± 0.05 Pg C yr^{-1}, Supplementary Table 3). Secondly, the hybrid approach was applied by considering observations from three consecutive years (see methods). This second sensitivity analysis also suggested a comparable increase in the decadal variability (to 0.14 ± 0.02 Pg C yr^{-1}, Supplementary Fig. S1). Overall, these two sensitivity analyses confirmed the robustness of the amplitude of the decadal variability suggested by the hybrid approach (Table 1). In contrast, the amplitude of the year-to-year variability was less robust because of insufficient data to constrain the hybrid approach on a yearly basis, especially in the 1990s (see Supplementary information).

Constraints on the regional ocean CO$_2$ sink

The regional ocean CO$_2$ sinks were constrained by applying the same hybrid approach but separately for three latitude bands, using only the observations in the North (>30°N), Tropics (30°S to 30°N), or South (<30°S) to constrain the regional ocean CO$_2$ sink simulated by NEMO-PlankTOM12.1 (Fig. 1b–d). The hybrid approach substantially modified the simulated ocean CO$_2$ sink in the mid- and high-latitude regions, particularly in the South, but with the Tropics remaining similar to the original NEMO-PlankTOM12.1 results. The hybrid approach increased the decadal variability simulated by NEMO-PlankTOM12.1 in the North and South regions (Supplementary Table 2).

In the North, where there are more SOCAT observations, the hybrid approach barely modified the mean ocean CO$_2$ sink simulated by NEMO-PlankTOM12.1. However, in the South, where there are fewer observations, the hybrid approach increased the mean ocean CO$_2$ sink simulated by NEMO-PlankTOM12.1 by 44% in the period 2000–2022. The hybrid approach applied at every 5° of latitude to constrain the mean climatological ocean CO$_2$ sink during 2000–2022 (rather than its annual values) shows that the mismatch between the model and the fCO$_2$ observations in the 40–60°S band could be the main cause of the underestimation of the ocean CO$_2$ sink in the South (Fig. 2). Note that it is the Southern region that has the most influence on the global ocean CO$_2$ sink.


Fig. 2 | Latitudinal mean ocean CO$_2$ sink averaged between 2000 and 2022. Positive values denote a sink for CO$_2$. The thick black line represents NEMO-PlankTOM12.1 standard simulation, the thin black lines represent the perturbed simulations, and the red dots represent the hybrid approach with ±1σ (68%) confidence interval. On the *x* axis, latitudes highlighted in red have an unconstrained ocean CO$_2$ sink. Empty red dots are latitudes with an uncertain constrained ocean CO$_2$ sink (see methods).

Decadal trends of the global ocean CO$_2$ sink

In the 1990s and 2000s, the hybrid approach enhanced the decadal trends simulated by NEMO-PlankTOM12.1, bringing the trends closer to those suggested by the fCO$_2$-products. In the 1990s, the hybrid approach decreased the NEMO-PlankTOM12.1 simulated trend from 0.02 to -0.19 ± 0.17 Pg C yr^{-1} decade^{-1}, to a value with the same sign and within the range of the fCO$_2$-product ensemble trend of -0.12 ± 0.35 Pg C yr^{-1} decade^{-1}. In the 2000s, the hybrid approach increased the simulated trend from 0.27 to 0.80 ± 0.21 Pg C yr^{-1} decade^{-1}, to a value also closer to and within the range of the fCO$_2$-product ensemble of 0.71 ± 0.38 Pg C yr^{-1} decade^{-1} (Fig. 3, Table 1).

In the 2010s, the hybrid approach decreased the simulated trend by NEMO-PlankTOM12.1 from 0.53 to 0.44 ± 0.15 Pg C yr^{-1} decade^{-1}, which is below the strong decadal trend of 0.68 ± 0.19 Pg C yr^{-1}
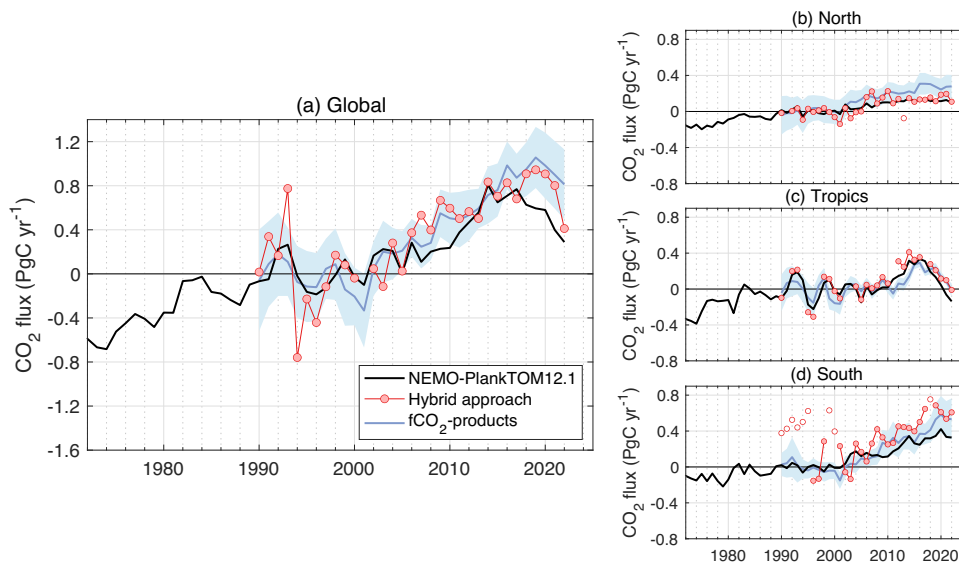
Fig. 3 | Anomalies of the ocean CO_2 sink constrained at global scale and by latitude bands between 1990 and 2022. a The global ocean is divided into three latitudinal bands: **b** North (>30°N), **c** Tropics (30°N–30°S), and **d** South (<30°S). The black line represents NEMO-PlankTOM12.1 standard simulation, the red line with the dots represents the hybrid approach, and the blue line represents the fCO₂-products. The fCO₂-product estimate is shown with ±1σ. For each time series, the long-term mean between 1990 and 1999 was removed to focus on the variability of the ocean CO_2 sink. fCO₂-product data credit: Global Carbon Budget 2023, licensed under Creative Commons Attribution 4.0 International (https://creativecommons.org/licenses/by/4.0/deed.en), no changes were made.

decade⁻¹ suggested by the fCO₂-product ensemble, but above the decadal trend of 0.34 ± 0.08 Pg C yr⁻¹ decade⁻¹ suggested by the GOBMs ensemble. As a consequence, the trend between 2000 and 2022 from the hybrid approach (0.42 ± 0.06 Pg C yr⁻¹ decade⁻¹) lies between the trend simulated by NEMO-PlankTOM12.1 and the GOBM ensemble (0.28 ± 0.05 Pg C yr⁻¹ decade⁻¹), and that suggested by the fCO₂-product ensemble (0.54 ± 0.13 Pg C yr⁻¹ decade⁻¹). However, unlike the GOBM and fCO₂-product ensembles where the growth is similar between the two decades, the trend in the hybrid approach is made of a decade of strong growth (in the 2000s) followed by a decade of weak growth (the 2010s). The distinct decadal trend variations between the 2000s and the 2010s suggested by the hybrid approach are robust to different configurations of the original model and to the choice of perturbed parameters (see methods). In comparison, only two out of seven fCO₂-products suggest that the trend in the 2000s should be higher than the trend in the 2010s over the global ocean.

Origin of the discrepancy among estimates

The differences in the decadal trends for the 2010s among the hybrid approach, the NEMO-PlankTOM12.1 and the fCO₂-products were mostly associated with the mid- and high-latitude regions (Fig. 3). Further investigation to determine the origin of the discrepancy was conducted, first by scrutinising estimates in the North where the density of SOCAT observations was the highest. This region encompasses 17% of the global ocean area. Because of the higher density of observations in the North compared with other latitudes, it is possible in this region to compare the trends in ocean CO_2 flux in areas that are generally well-sampled to those in areas that are poorly sampled. A similar analysis cannot be done for the South because of the insufficient data coverage. In the North, the hybrid approach and average GOBMs produce lower trends compared to the average of the fCO₂-products (Fig. 3b).

The SOCAT observations, by themselves, do not confirm the existence of a strong decadal trend in the 2010s in the North. The strong decadal trend in the ocean CO_2 flux estimated by the fCO₂-products is primarily driven by diverging trends between the CO_2 fugacity at the surface of the ocean compared to that in the atmosphere (ΔfCO_2)[36]. The SOCAT observations converted into ΔfCO_2 in

the North region between 2000 and 2019 show a positive and higher trend in the 2000s compared to the 2010s (Fig. 4). Similar temporal patterns were visible in the ΔfCO_2 data from the fCO₂-products subsampled to SOCAT sampling points, with a decadal trend in ΔfCO_2 in the 2000s significantly higher than in the 2010s (Kruskal–Wallis test, p value < 0.01), as expected. However, when not subsampled, the fCO₂-products suggested a decadal trend in ΔfCO_2 in the 2000s that is not significantly higher than in the 2010s (Kruskal–Wallis test, p value = 0.14), with an overlap in the estimated uncertainties in the two decades, explaining the small differences in the CO_2 sink trend between the 2000s and 2010s. This is induced by the fact that three of the seven fCO₂-products suggested a greater trend in the 2010s compared to the 2000s, and a fourth fCO₂-product suggested a strong trend in both decades. In comparison, when subsampled or not subsampled, the GOBMs suggested a decadal trend in ΔfCO_2 in the 2000s significantly higher than in the 2010s (Kruskal–Wallis tests, p value < 0.001). In addition, the decadal trend in ΔfCO_2 in the North during the 2010s is significantly higher in the fCO₂-product ensemble than in the GOBMs ensemble (Kruskal–Wallis test, p value < 0.01). The differences between the subsampled and not subsampled results suggest that different extrapolation methods outside of data-rich regions could account for the higher decadal trend in ocean CO_2 sink in the North over the 2010s in the fCO₂-products ensemble compared to the GOBMs ensemble and the hybrid approach (Fig. 3b, Supplementary Table 2).

Within the four fCO₂-products that suggested a strong positive decadal trend in ΔfCO_2 in the 2010s in the North, the ocean area associated with the highest trend values overlaps the northern Pacific Ocean (Fig. 5a) which was undersampled in the 2010s (white areas in Fig. 5b). In quantitative terms, these four fCO₂-products suggested that the Pacific Ocean contributed 0.04 Pg C yr⁻¹ decade⁻¹ of the 2010s trend in the North, while the other three fCO₂-products (below the fCO₂-product average) suggested that the Pacific Ocean had a negative trend in the 2010s (−0.01 Pg C yr⁻¹ decade⁻¹), as simulated by the GOBM average.

In addition to the extrapolation problems in the undersampled northern regions mentioned above, on a global scale, the estimate of the positive trend in the 2010s from the fCO₂-product ensemble has

been revised downwards in successive publications of the global carbon budget analysis between 2021 and 2023, while their trends for the 1990s and 2000s have remained relatively similar (Fig. 6). For each of the global carbon budget analyses published between 2021 and 2023, the fCO$_2$-product ensemble average has always been produced from seven estimates. However, two of the seven fCO$_2$-products were introduced, replacing previously submitted products that were not updated, and five were slightly updated. Among these five fCO$_2$-products, on average, the 2010 trend between the 2021 and 2023 publications decreased by −0.05 Pg C yr^{-1} decade^{-1}. Thus, it was mainly the turnover in the last two fCO$_2$ products between 2021 and 2023 that led to a visible decrease in the ensemble average of −0.25 Pg C yr^{-1} decade^{-1} for the 2010 trend. Consequently, the downward revision observed for the observation-based estimate was mainly due to a change in two fCO$_2$-product methodologies and, to a lesser extent, to the annual updates of the SOCAT database and fCO$_2$-product

Fig. 4 | Decadal trends in ΔfCO$_2$ in the North (>30°N, excluding the Arctic Ocean). Comparison of the measured decadal trend in ΔfCO$_2$ from SOCAT (green dots) with that of the fCO$_2$-product ensemble (blue box-plots and dots) and of the GOBM ensemble (grey box-plots and dots). The box-plots display: the median, the lower and upper quartiles, and the minimum and maximum values that are not outliers. The trends are calculated from median annual values for the North region. On the left, fCO$_2$-products and GOBMs were subsampled at SOCAT locations, while on the right, they were not subsampled, and the value for the North region as a whole is shown. fCO$_2$-product and GOBM data credit: Global Carbon Budget 2023, licensed under Creative Commons Attribution 4.0 International (https://creativecommons.org/licenses/by/4.0/deed.en), no changes were made.

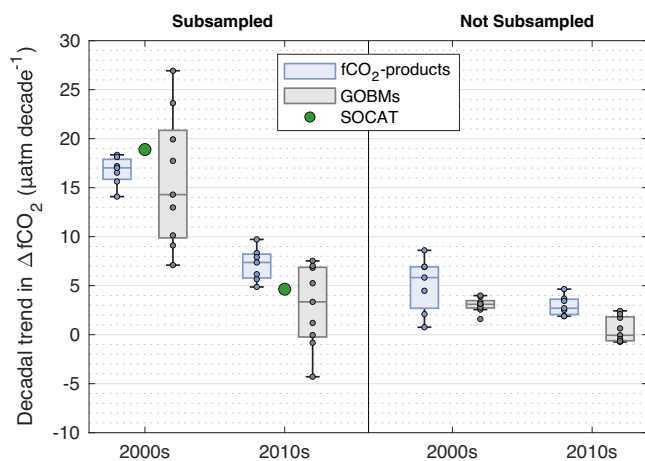methods, suggesting that the trend of the 2010s estimated with the fCO$_2$-products is not robust at this stage.

Discussion

Over the 1990s and 2000s, the ocean CO$_2$ sink experienced a well-documented stagnation in the 1990s[14,19,20,31] and a reinvigoration trend in the 2000s[37], but the amplitude of these decadal trends is uncertain. Several studies have shown that the trends were present in many GOBMs but with amplitude much lower than in the fCO$_2$-products[19,20]. Results from the hybrid approach presented here confirm that the amplitude of decadal trends in the ocean CO$_2$ sink is underestimated by NEMO-PlankTOM12.1 and the other GOBMs and suggest decadal trend values close to those estimated using fCO$_2$-products for these two decades (Table 1).
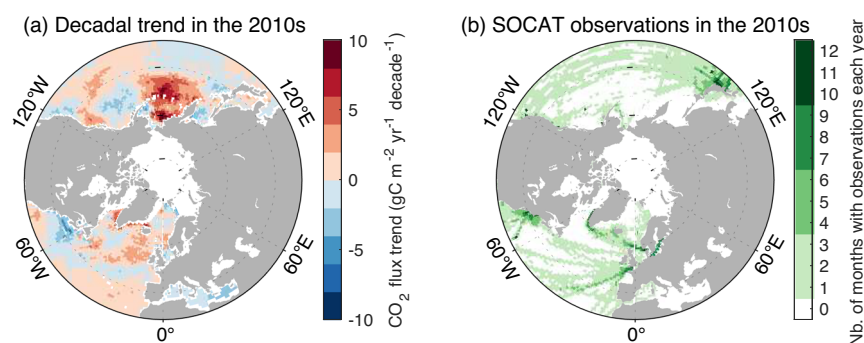
For the 2010 decade, the hybrid approach suggests a lower decadal trend in the ocean CO$_2$ sink compared to the 2000s, with a value closer to that simulated by most GOBMs and lower than that suggested by the fCO$_2$-products ensemble. However, both GOBMs and fCO$_2$-products ensembles suggest similar trends between 2000s and 2010s, while the hybrid approach (including the sensitivity analyses, Supplementary Table 3) consistently produced a higher trend in the 2000s compared to the 2010s.

Our results suggest that the estimate of the ocean CO$_2$ sink trend in the 2010s by the fCO$_2$-product ensemble is overestimated and sensitive to the availability and distribution of fCO$_2$ observations. Over the last three annual updates of global carbon budgets[2,38,39], the 2010s trend estimated from the ensemble of available products has decreased by 14% each year (Fig. 6). This supports our finding of an overestimated trend in the 2010s ocean CO$_2$ sink from the fCO$_2$-products ensemble, which is adjusted downwards as new data become available. In addition, the replacement of two members of the fCO$_2$-product ensemble by a hybrid approach along the same lines as presented here[32,40] and by a revised fCO$_2$-product aimed at improving the retrieval of the ocean CO$_2$ sink trend[41] have led to this downward revision of the 2010s trend in the latest ensemble.

The ±1σ uncertainty provided for the hybrid results reflects the capacity of the hybrid approach to constrain the annual ocean CO$_2$ sink given the availability and distribution of the fCO$_2$ observations. The annual uncertainty is then propagated to the decadal trend. The trend for the period 2000–2022 is better constrained than the individual ten-year trends, since the longer period naturally filters out short-term variability. Nevertheless, sensitivity tests suggest that additional uncertainty to the model set up influences the exact value of the trends, but not the overall patterns, and in particular the trend in the 2010s which is systematically lower than the trend in the 2000s in all sensitivity tests performed, and also systematically lower than the


Fig. 5 | Spatial distribution of anomalies in decadal trends of the ocean CO$_2$ sink estimated by four fCO$_2$-products in the North, and location of observations, for the period 2010–2019. a The anomalies represent the difference between the average estimate from the four fCO$_2$-products with the highest trends during this decade, and the average of all seven fCO$_2$-products. **b** Median number of months with SOCAT observations available each year between 2010 and 2019. fCO$_2$-product data credit: Global Carbon Budget 2023, licensed under Creative Commons Attribution 4.0 International (https://creativecommons.org/licenses/by/4.0/deed.en), no changes were made.
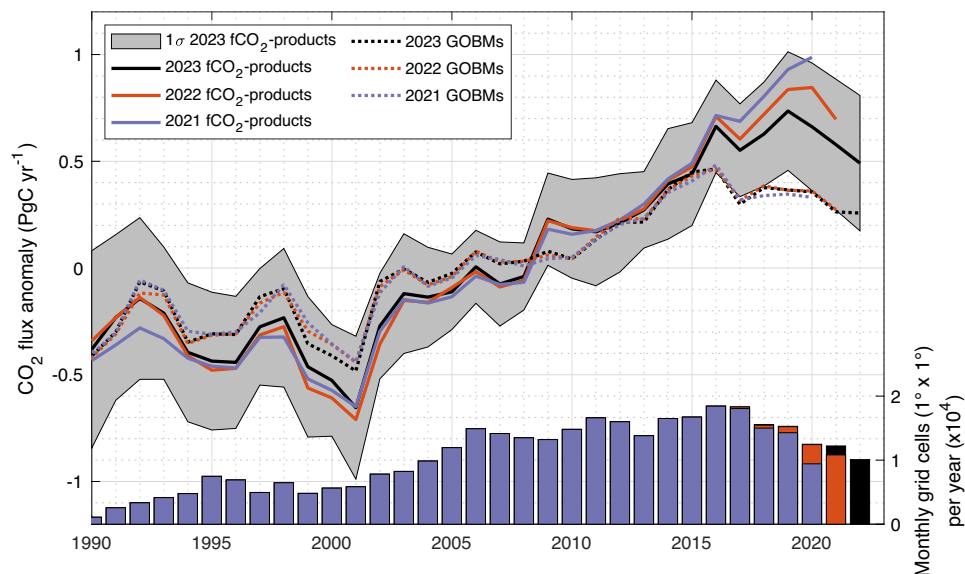
Fig. 6 | Changes in fCO₂-product estimates over the last three updates of the global carbon budget analysis. The last update of the fCO₂-product estimate was in 2023 (black line and grey shade). The previous two estimates were in 2022 (orange) and 2021 (blue). The left y axis represents the global CO_2 flux anomaly (for each time series the long-term mean between 1990 and 2020 was removed). GOBM estimates for the same three global carbon budget updates are also shown in dotted lines. The bar chart at the bottom represents the number of annual observations in the SOCAT database, for each annual version of SOCAT (v2021, v2022, and v2023; using the same colour code as for the line). fCO₂-product and GOBM data credit: Global Carbon Budget 2023, licensed under Creative Commons Attribution 4.0 International (https://creativecommons.org/licenses/by/4.0/deed.en), no changes were made.

fCO₂-products ensemble for that decade. Our analysis demonstrates the importance of regular updates and efforts to collect fCO₂ observations as part of SOCAT[17], as well as regular evaluations of data products, including fCO₂-products and new hybrid methodologies[42,43].

Differences between NEMO-PlankTOM12.1, the hybrid approach, and the fCO₂-products ensemble for the 2010s decadal trend are mostly visible in the mid- and high-latitude regions of both hemispheres (Fig. 3). Our results suggest that some fCO₂-products overestimate the decadal trend of the 2010s in northern regions where there are few observations. In the northern latitudes, where the availability of measurements is highest, the fCO₂-product ensemble gives a decadal trend in the 2000s not significantly different from that of the 2010s (Fig. 4). Four fCO₂-products suggest a growing or strong trend during the 2010s, contrary to the fCO₂ observations alone, which is explained here by their strong trends in areas that were undersampled during the 2010s (Fig. 5). Hence, we hypothesise that methodological issues in some fCO₂-products could lead to an unrealistic amplification of the ocean CO_2 sink trend in the 2010s. In addition, the ocean CO_2 sink in the northern region is also more influenced by coastal processes than the southern region, which despite their importance remain uncertain[44–48]. Consequently, in the northern region, the way in which coastal fCO₂ observations are considered by the various fCO₂-products could induce some of the discrepancies among fCO₂-products. This would partly explain the lack of coherence between the GOBMs and the fCO₂-products over this recent decade[2,6,22,23].

In the Southern Ocean, our hybrid approach suggests that existing fCO₂ measurements could corroborate a strong and positive decadal trend in this region in the 2010s, and more generally between 2000–2022. However, the paucity of fCO₂ measurements in the Southern Ocean impedes our ability to evaluate the decadal trend in this region using observations only[42]. Nevertheless, our estimate of the decadal trend of the Southern Ocean CO_2 sink in the period 2000–2022 is within the range of the fCO₂-product ensemble (Supplementary Table 2). But the uncertainties associated with our hybrid approach are the largest in the Southern Ocean. Moreover, recent studies showed that undersampling could be responsible for strong biases in fCO₂ products in that region[43].

The hybrid approach presented here suggests that GOBMs underestimate the amplitude of the decadal variability of the ocean CO_2 sink over the past three decades by about $38 \pm 8\%$, and that the value should be within the range suggested by fCO₂-products (Table 1). Although our hybrid approach always suggests an underestimation of the decadal variability by GOBMs, the exact value is sensitive to the specific model configuration (Supplementary Table 3). The underestimation of the decadal variability by GOBMs was mostly reported in the North and South regions[2,20]. These deficiencies in the mid- and high-latitude regions have been related to the coarse resolution of the ocean circulation models[2], the generally poor representation of the seasonality of fCO₂ in these regions[49–51], and / or insufficient variability in simulated mode-water formation[52]. A possible overestimation of the decadal variability by fCO₂-products by 30% has been postulated before[42] because of undersampling of surface ocean fCO₂, mostly in the Southern Ocean[43,53,54]. Results from our hybrid approach also show there are remaining issues in CO_2 flux estimates of undersampled regions by fCO₂-products, but suggest that the amplitude of decadal variability is nevertheless greater than that estimated by GOBMs.

Finally, for the mean ocean CO_2 sink, the hybrid approach returns a higher mean CO_2 sink than NEMO-PlankTOM12.1 in the Southern Ocean because it corrects a consistent bias of overestimation of the surface ocean fCO₂ (Supplementary Fig. S2). Studies based on emergent constraint properties[55–57], and thorough assessments of the ability of GOBMs to simulate the Southern Ocean CO_2 sink[58], have also suggested that the current generation of models underestimates the global ocean CO_2 sink due to a deficient representation of ocean circulation in the Southern Ocean. The CO_2 outgassing from river fluxes, which is not included in NEMO-PlankTOM12.1 and the other GOBM simulations, could also explain the bias. River outgassing in the Southern Ocean has been estimated at 0.32 Pg C yr⁻¹ but with a high degree of uncertainty[2,59]. This bias would not affect the estimates of variability and trends, which are mainly driven by perturbation of surface ocean dynamics and atmospheric CO_2 concentration resulting from climate trends and variability (particularly winds) and by the evolution of atmospheric CO_2[6,16,60]. However, this means that our hybrid approach is less robust in estimating the mean ocean CO_2 sink

than the variability and trend of this sink, because the mean ocean CO_2 sink also depends on mixing between the surface ocean and the deep ocean[10], a process that is weakly constrained when only using surface fCO_2 observations, as is the case in the hybrid approach. Further work, in particular the use and/or assimilation of ocean interior carbon data[24,28,29], would be better suited to constrain the mean ocean CO_2 sink.

Our hybrid approach has shown that estimates of the temporal evolution of the ocean CO_2 sink can be reconciled, providing a well-constrained estimate of a significant growth in the ocean CO_2 sink between 2000 and 2022 of 0.42 ± 0.06 Pg C yr^{-1} decade^{-1}, corresponding to a growth of 1.0 Pg C yr^{-1} over those 23 years. Results from our hybrid approach show similarities and discrepancies with the CO_2 sink estimates from both GOBMs and fCO_2-products. Therefore, our analysis validates the global carbon budget approach to evaluate the ocean CO_2 sink by combining the data-based and process-model estimates[2]. Moreover, it confirms the importance of high-density fCO_2 observations, which are notably lacking in the Southern Ocean, for informing the fCO_2-products and our hybrid approach. It suggests that fCO_2-products could be further improved by scrutinizing the extrapolation of observations in the 2010s, which are evolving over the different versions released, in order to understand differences among fCO_2-products and then help improve the products.

Within the limits of the hybrid approach, a trend of 0.28 ± 0.13 Pg C yr^{-1} decade^{-1} in the total land CO_2 sink (including natural fluxes and emissions from land-use changes) can be inferred based on our estimate of the trend in the ocean CO_2 sink for 2000–2022, corresponding to a growth of 0.6 Pg C yr^{-1} over those 23 years. This result was obtained by adding to and subtracting from our estimate of the ocean CO_2 sink, global carbon budget estimates for the growth rate of atmospheric CO_2 and CO_2 emissions from fossil fuels (taking into account cement carbonation, detailed in the Supplementary information)[2]. Our estimated trend in the total land CO_2 sink lies between the 0.43 ± 0.20 Pg C yr^{-1} decade^{-1} trend estimated by the global carbon budget analysis[2] and the trend of 0.07 ± 0.14 Pg C yr^{-1} decade^{-1} that would be obtained with the ocean CO_2 sink estimate from the fCO_2-products alone. Therefore, the land trend inferred from fCO_2 observations suggests either an overestimation of the increasing trend in the simulated land CO_2 sink by Dynamic Global Vegetation Models, an overestimation of the decreasing trend in CO_2 emissions from land-use changes by bookkeeping approaches used in the global carbon budget analysis (which might be increasing), or both[2]. The latter includes the possibility that emissions from land-use changes were stable or even increased during 2000–2022, which is plausible given the large uncertainty in land-cover change data and in management processes[2]. Our results demonstrate that ocean observations can constrain trends in land CO_2 fluxes, and that results are limited by the availability of fCO_2 observations.

Methods
Amplitude of the decadal variability and decadal trend estimates
The amplitude of the decadal variability was estimated as the standard deviation of the decadal component of the annual ocean CO_2 sink time series. The decadal components were extracted from the time series using the following signal decomposition methodology[52]: (i) the linear trend and long-term mean were removed to isolate the temporal variability, (ii) the decadal component of this detrended time series was obtained by filtering this time series with a 10-year Hanning window. The Hanning window is a filtering function with a 'bell-shaped' curve used to smooth the signal by emphasizing the feature near the center of the window. All uncertainty ranges are reported here with a $\pm 1\sigma$ (68%) confidence interval, as in global carbon budget analysis[2].

The decadal trends of ocean CO_2 sink and ΔfCO_2 were estimated with the Theil-Sen slope estimator[61,62]. To calculate ΔfCO_2, the

atmospheric CO_2 mole fraction (xCO_2) used in the global carbon budget analysis (data from the U.S. National Oceanic and Atmospheric Administration, Global Monitoring Laboratory[63]) is first converted to pCO_2 taking into account the atmospheric surface pressure corrected for the vapour pressure of seawater (P_{atm}), and then to fCO_2 with a fugacity coefficient estimated as follows[64],

$$fCO_2 = pCO_2 \cdot \exp\left(P_{atm} \cdot \frac{\left(B + (1 - xCO_2)^2 \cdot 2\delta\right)}{(R \cdot T)}\right) \quad (1)$$

where T is the sea surface temperature (in Kelvin, from OISST1.2[65]), B and δ are the virial coefficients for carbon dioxide[66] and R is the gas constant[64]. The necessary sea surface salinity data come from EN4 (EN.4.2.2.g10[67]), and the surface atmospheric pressure data come from ERA5[68].

For the GOBM and fCO_2-product ensembles (from the global carbon budget analysis), the amplitude of the decadal variability, and the decadal trends were calculated for each member of the ensemble. The mean ensemble values are reported with their standard deviation. For the hybrid approach, the amplitude of the decadal variability, and decadal trends were calculated with the annual constrained values. An estimate of the standard deviation around these values was obtained by re-calculating 10,000 times these estimates with annual ocean CO_2 sink values that had been randomly selected (from a uniform distribution) within the estimated confidence intervals of the annual constrained value.

Description and evaluation of the NEMO-PlankTOM12.1 model
The NEMO-PlankTOM12.1 model consists of a global ocean general circulation model, NEMO v3.6, with an embedded biogeochemical model, PlankTOM12.1, forced by atmospheric meteorological data from the NCEP reanalysis product[30].

NEMO-PlankTOM12.1 used the NEMO model[69] in its global configuration on the ORCA tripolar grid, with a longitudinal resolution of 2° and an average latitudinal resolution of 1.5°, the latter being enhanced up to 0.3° in the tropics and at high latitudes, and a temporal resolution of 96 min. This physical ocean model comprises a total of 31 vertical z levels with a vertical resolution of 10 m for the first 100 m, decreasing progressively to a resolution of 500 m at a depth of 5 km. The NEMO model is based on the Navier-Stokes equations and a non-linear equation of state. It explicitly calculates vertical mixing using a turbulent closure model. Subgrid-scale eddy-induced mixing is represented with a parameterisation[70]. NEMO is coupled to the Louvain-La-Neuve sea ice model (LIM[71]).

The PlankTOM12.1 biogeochemical model simulates the full marine cycles of carbon, oxygen, phosphorus and silicon, and simplified cycles for iron and nitrogen. This biogeochemical model was obtained by merging two versions of the PlankTOM model series, which had been developed in parallel, one focused on the role of jellyfish[72], and one focused on the role of pteropods[73]. This version has been used in the global carbon budget analysis 2022[39] and 2023[2]. Its ecosystem component is based on the representation of 12 Plankton Functional Types (PFTs), including six phytoplankton, five zooplankton and one bacteria. Spatiotemporal variations in PFT concentrations are induced by the simulated response of each PFT to environmental conditions, including temperature, nutrient availability, light, and interactions between PFTs. PlankTOM12.1 explicitly represents dissolved organic carbon and two size classes of particulate organic carbon, one small and one large. These components are influenced by the particle aggregation process, and the large particles are also influenced by the effect of mineral ballasting. Simulated dissolved inorganic carbon and alkalinity are influenced by air-sea exchanges of CO_2, calcification (production and dissolution), primary production, and remineralisation of organic matter (grazing by zooplankton and

remineralisation by bacteria). The alkalinity is also influenced by denitrification. A full description of PlankTOM12.1 biogeochemistry has been published[34]. Model simulations are too short to fully represent the input of river fluxes and their subsequent outgassing of CO_2 in the open ocean. Instead, constant river fluxes of dissolved and organic carbon and nutrients are prescribed as input at the location of river mouth, and corresponding fluxes are removed from the bottom sediments to conserve mass. The version of the NEMO-PlankTOM12.1 code used here is the same as that used in the latest global carbon budget analysis, forced with NCEP reanalysis. For this, the model was spun up first from 1750 to 1947 with a 30 years (1948–1977) climatological annual cycle of atmospheric forcing from the NCEP reanalysis product, followed by the use of annual forcing from 1948 until 2022.

The validation of this model version was first carried out by ensuring that the simulated surface chlorophyll-*a* concentration, primary production, and nutrient distributions were reasonably simulated, as in previous model versions[74]. Second, we examined the RMSE relative to the SOCAT gridded fCO_2 observations and the temporal variability of the ocean CO_2 sink between 1990–2022. These two variables are used to evaluate GOBMs in the global carbon budget analysis. The RMSE value associated with NEMO-PlankTOM12.1 (38.5 µatm) is within the range of GOBMs used in the global carbon budget analysis (31.3 µatm–45.0 µatm). The interannual and decadal variabilities of the ocean CO_2 sink from NEMO-PlankTOM12.1 are also comparable to the other GOBMs of the global carbon budget (Supplementary Table 1), and the simulated mean ocean CO_2 sink in the 1990s (1.91 Pg C yr^{-1}) falls within the observational range (1.5 to 2.9 Pg C yr^{-1})[3].

Finally, the performance of NEMO-PlankTOM12.1 was evaluated with the metrics adopted by the global carbon budget in 2023: the simulated Atlantic Meridional Overturning Circulation, Southern Ocean sea surface salinity, the Southern Ocean stratification index, and surface ocean Revelle factor. The values simulated by NEMO-PlankTOM12.1 are within the range of the values simulated by the other GOBMs and are close to the observed values, with the exception of the Southern Ocean stratification index for which NEMO-PlankTOM12.1 has the lowest value but remains within comparable range (Supplementary Fig. S3).

Hybrid approach

A hybrid approach is developed to constrain the annual ocean CO_2 sink simulated by the NEMO-PlankTOM12.1 model on the basis of the model-observation mismatch for surface fCO_2. This approach is not implemented to significantly improve the model-observation mismatch, but to correct for annual biases in the simulated ocean CO_2 sink, after the standard simulation is done, thus providing an adjusted annual estimate with uncertainty. This methodology has been previously used to constrain the climatological ocean primary production[33] and air-sea fluxes of N_2O[34] and CCl_4[35]. Because there are more observations available for surface fCO_2 observations than for N_2O or CCl_4, this hybrid approach can be performed annually.

The surface fCO_2 observations used here are the ones compiled within the SOCAT v2023 database[75]. This database is a gridded product (1° × 1°) with a monthly temporal resolution. All monthly model outputs used here were regridded to the same spatial resolution as SOCAT.

First, to perform this hybrid approach, four perturbed simulations of NEMO-PlankTOM12.1 are produced with higher average MSEs (between the model and SOCAT observations, with equal weight given to each gridded observational data) over the simulated period, and lower or higher annual ocean CO_2 sink. These perturbed simulations range from 1.3 Pg C yr^{-1} to 3.2 Pg C yr^{-1} on average during 2000–2022, and span the expected range suggested by the global carbon budget analysis (i.e., 2.6 ± 0.4 Pg C yr^{-1} on average, with

individual years ranging from 1.8 Pg C yr^{-1} to 3.0 Pg C yr^{-1}). They are obtained by perturbing model parameters, changing the half-saturation constant for bacteria remineralisation of organic carbon from 5×10^{-6} mol L^{-1} to 18×10^{-6} mol L^{-1}. This parameter was chosen because of its strong influence on the ocean CO_2 sink that is relatively uniform over the entire ocean. Second, for each year, a plot of the annual MSE values (on the y axis) against the annual ocean CO_2 sink (x axis) associated with the four model simulations (the optimal simulation and the four perturbed simulations) is produced and a cubic function is fitted through these data points. Third, the constrained annual ocean CO_2 sink is estimated by finding the local minimum (turning point) associated with the concave upward section of the fitted cubic function. This local minimum corresponds to a theoretical model simulation with an annual ocean CO_2 sink that presents the smallest MSE (MSE_{min}). Note that if the fit did not have a local minimum the ocean CO_2 sink from this year is not constrained. Years with a constrained ocean CO_2 sink not within the range of the ocean CO_2 sink from the perturbed simulations are kept but considered uncertain values.

Finally, the ± 1σ (68%) confidence interval associated with the determined MSE_{min} value is estimated with this formula[33],

$$\frac{MSE_{68\%}}{MSE_{min}} = 0.468 \times \frac{n}{(n-2)} \times \sqrt{\left(\frac{2(2n-2)}{n(n-4)}\right)} + \frac{n}{(n-2)} \quad (2)$$

where n is the number of gridded observational data points, and $MSE_{68\%}$ corresponds to the MSE value for theoretical model simulations located at the borders of the confidence interval, and their associated annual ocean CO_2 sink is estimated by using the cubic function (i.e., determined where $f(x) = MSE_{68\%}$ with x being the annual ocean CO_2 sink). See Supplementary Fig. S4 for a graphical interpretation of this hybrid approach. The global performance of the hybrid approach is evaluated with the two standard metrics used by the global carbon budget annual analysis[2]—i.e., the RMSE relative to the SOCAT fCO_2 observations and the estimated temporal variability of the ocean CO_2 sink (results in Supplementary Table 1).

The hybrid approach reduced the RMSE between NEMO-PlankTOM12.1 and SOCAT observations (the RMSE values associated with the perturbed simulations, PlankTOM12.1 and the hybrid approach are 39.9 µatm, 38.5 µatm and 38.0 µatm, respectively). For comparison, the GOBMs and fCO_2-products listed in the global carbon budget analysis in 2023 had mean RMSE values of 39.0 µatm and 20.3 µatm, respectively. Note that fCO_2-products were based on SOCAT observations and are therefore not independent, which explains their lower RMSE values.

This hybrid approach is also used to constrain regional ocean CO_2 sink values at three latitude bands, and at every 5° of latitude. For this regional analysis, the number of available SOCAT observations is lower, therefore only the quadratic function is used to provide wider confidence intervals and reflect the lower confidence in the constrained values.

We performed sensitivity analyses to test the robustness of our results to the choice of perturbed model parameters and model configurations. The perturbed simulations were repeated with parameters of phytoplankton respiration, and with a combination of both bacterial half-saturation and phytoplankton respiration. The model configuration was changed by using ERA5 reanalysis as weather-forcing data. In total, we thus have applied the hybrid approach to six different set ups, with three choices of perturbation parameters and two choices of forcing configurations (Supplementary Fig. S5). Regardless of the parameter and configuration used, the results consistently produced the lowest trend in the 1990s, and a higher trend in the 2000s than in the 2010s, although the exact trends within each decade varied (Supplementary Fig. S6 and Supplementary Table 3). We show here results of the model forced with NCEP, which has a lower RMSE (38.5 µatm)

compared to the configuration forced with ERA5 (40.0 µatm), and the perturbation of the half-saturation constant of bacterial remineralisation, which produces changes in fCO_2 that are more uniform across the ocean.

Finally, we also carried out an analysis to assess the influence of the annual application of the hybrid approach by considering, instead, three consecutive years. Therefore, rather than using a series of plots of the annual MSE value against the annual ocean CO_2 sink (e.g., Supplementary Fig. S4), we used a series of plots of the 3-year MSE value against the 3-year average ocean CO_2 sink.

Data availability
Data from NEMO-PlankTOM12.1 and hybrid approach generated in this study have been deposited: https://osf.io/2kzps/?view_only= 6ad809f1887342a0a19907e40a33e7cf. All other data is publicly available and instructions on how to access it are published on the following GitHub repository: https://github.com/nmayot/hybrid_approach.

Code availability
The code used to perform the analysis is publicly available on a GitHub repository: https://github.com/nmayot/hybrid_approach.

References
1. Canadell, J. G. et al. Global carbon and other biogeochemical cycles and feedbacks. In: *Climate Change 2021: The Physical Science Basis. Contribution of Working Group I to the Sixth Assessment Report of the Intergovernmental Panel on Climate Change* (eds. Masson-Delmotte, V. et al.) 673–816 (Cambridge University Press, Cambridge, UK, NY, USA, 2021).
2. Friedlingstein, P. et al. Global carbon budget 2023. *Earth Syst. Sci. Data* **15**, 5301–5369 (2023).
3. Ciais, P. et al. Carbon and other biogeochemical cycles. In: *Climate Change 2013: The Physical Science Basis. Contribution of Working Group I to the Fifth Assessment Report of the Intergovernmental Panel on Climate Change* 465–570 (Cambridge University Press, Cambridge, United Kingdom and New York, NY, USA, 2013).
4. Sarmiento, J. L. & Gruber, N. Ocean biogeochemical dynamics. i–iv. Princeton University Press (2006).
5. McKinley, G. A., Fay, A. R., Eddebbar, Y. A., Gloege, L. & Lovenduski, N. S. External forcing explains recent decadal variability of the ocean carbon sink. *AGU Adv.* **1**, e2019AV000149 (2020).
6. Gruber, N. et al. Trends and variability in the ocean carbon sink. *Nat. Rev. Earth Environ.* **4**, 119–134 (2023).
7. Bunsen, F., Hauck, J., Nerger, L. & Torres-Valdés, S. Ocean carbon sink assessment via temperature and salinity data assimilation into a global ocean biogeochemistry model. *EGUsphere* 1–48 https://doi.org/10.5194/egusphere-2024-1750 (2024).
8. Le Quéré, C. et al. Two decades of ocean CO2 sink and variability. *Tellus B: Chem. Phys. Meteorol.* **55**, 649–656 (2003).
9. Denman, K. L. et al. Couplings between changes in the climate system and biogeochemistry. In: *Climate Change 2007: The Physical Science Basis. Contribution of Working Group I to the Fourth Assessment Report of the Intergovernmental Panel on Climate Change* 499–588 (Cambridge University Press, Cambridge, United Kingdom and New York, NY, USA, 2007).
10. Orr, J. C. et al. Estimates of anthropogenic carbon uptake from four three-dimensional global ocean models. *Glob. Biogeochem. Cycles* **15**, 43–60 (2001).
11. Keeling, R. F., Piper, S. C. & Heimann, M. Global and hemispheric CO2 sinks deduced from changes in atmospheric O2 concentration. *Nature* **381**, 218 (1996).
12. Manning, A. & Keeling, R. F. Global oceanic and land biotic carbon sinks from the Scripps atmospheric oxygen flask sampling network. *Tellus B: Chem. Phys. Meteorol.* **58**, 95–116 (2006).
13. Gloor, M. et al. A first estimate of present and preindustrial air-sea CO2 flux patterns based on ocean interior carbon measurements and models. *Geophys. Res. Lett.* **30**, 10-1-10–10-1-14 (2003).
14. Le Quéré, C. et al. Saturation of the Southern ocean CO2 sink due to recent climate change. *Science* **316**, 1735–1738 (2007).
15. Lenton, A. & Matear, R. J. Role of the Southern Annular Mode (SAM) in Southern Ocean CO2 uptake. *Glob. Biogeochem. Cycles* **21**, GB2016 (2007).
16. Le Quéré, C. et al. Trends in the sources and sinks of carbon dioxide. *Nat. Geosci.* **2**, 831–836 (2009).
17. Bakker, D. C. E. et al. A multi-decade record of high-quality *f*CO2 data in version 3 of the Surface Ocean CO2 Atlas (SOCAT). *Earth Syst. Sci. Data* **8**, 383–413 (2016).
18. Sabine, C. L. et al. Surface Ocean CO2 atlas (SOCAT) gridded data products. *Earth Syst. Sci. Data* **5**, 145–153 (2013).
19. DeVries, T. et al. Decadal trends in the ocean carbon sink. *Proc. Natl Acad. Sci.* **116**, 11646–11651 (2019).
20. Hauck, J. et al. Consistency and challenges in the ocean carbon sink estimate for the global carbon budget. *Front. Mar. Sci.* **7**, 571720 (2020).
21. Gruber, N. et al. The oceanic sink for anthropogenic CO2 from 1994 to 2007. *Science* **363**, 1193–1199 (2019).
22. Keppler, L., Landschützer, P., Lauvset, S. K. & Gruber, N. Recent trends and variability in the oceanic storage of dissolved inorganic carbon. *Glob. Biogeochem. Cycles* **37**, e2022GB007677 (2023).
23. Müller, J. D. et al. Decadal trends in the oceanic storage of anthropogenic carbon from 1994 to 2014. *AGU Adv.* **4**, e2023AV000875 (2023).
24. Zemskova, V. E., He, T.-L., Wan, Z. & Grisouard, N. A deep-learning estimate of the decadal trends in the Southern Ocean carbon storage. *Nat. Commun.* **13**, 4056 (2022).
25. DeVries, T. et al. Magnitude, trends, and variability of the global ocean carbon sink from 1985–2018. *Glob. Biogeochem. Cycles* **n/a**, e2023GB007780 (2023).
26. Brasseur, P. et al. Integrating biogeochemistry and ecology into ocean data assimilation systems. *Oceanography* **22**, 206–215 (2009).
27. Verdy, A. & Mazloff, M. R. A data assimilating model for estimating Southern Ocean biogeochemistry. *J. Geophys. Res.: Oceans* **122**, 6968–6988 (2017).
28. Carroll, D. et al. The ECCO-Darwin data-assimilative global ocean biogeochemistry model: estimates of seasonal to multidecadal surface ocean pCO2 and air-sea CO2 flux. *J. Adv. Model. Earth Syst.* **12**, e2019MS001888 (2020).
29. Li, H., Ilyina, T., Loughran, T., Spring, A. & Pongratz, J. Reconstructions and predictions of the global carbon budget with an emission-driven Earth system model. *Earth Syst. Dyn.* **14**, 101–119 (2023).
30. Kalnay, E. et al. The NCEP/NCAR 40-year reanalysis project. *Bull. Am. Meteorol. Soc.* **77**, 437–472 (1996).
31. Le Quéré, C., Takahashi, T., Buitenhuis, E. T., Rödenbeck, C. & Sutherland, S. C. Impact of climate change and variability on the global oceanic sink of CO2. *Glob. Biogeochem. Cycles* **24**, (2010).
32. Gloege, L., Yan, M., Zheng, T. & McKinley, G. A. Improved quantification of ocean carbon uptake by using machine learning to merge global models and pCO2 data. *J. Adv. Model. Earth Syst.* **14**, e2021MS002620 (2022).
33. Buitenhuis, E. T., Hashioka, T. & Quéré, C. L. Combined constraints on global ocean primary production using observations and models. *Glob. Biogeochem. Cycles* **27**, 847–858 (2013).
34. Buitenhuis, E. T., Suntharalingam, P. & Le Quéré, C. Constraints on global oceanic emissions of N2O from observations and models. *Biogeosciences* **15**, 2161–2175 (2018).
35. Suntharalingam, P. et al. Evaluating oceanic uptake of atmospheric CCl4: a combined analysis of model simulations and observations. *Geophys. Res. Lett.* **46**, 472–482 (2019).

36. Fay, A. R. et al. SeaFlux: harmonization of air–sea CO_2 fluxes from surface pCO_2 data products using a standardized approach. *Earth Syst. Sci. Data* **13**, 4693–4710 (2021).

37. Landschützer, P. et al. The reinvigoration of the Southern Ocean carbon sink. *Science* **349**, 1221–1224 (2015).

38. Friedlingstein, P. et al. Global carbon budget 2021. *Earth Syst. Sci. Data* **14**, 1917–2005 (2022).

39. Friedlingstein, P. et al. Global carbon budget 2022. *Earth Syst. Sci. Data* **14**, 4811–4900 (2022).

40. Bennington, V., Galjanic, T. & McKinley, G. A. Explicit physical knowledge in machine learning for ocean carbon flux reconstruction: the pCO2-residual method. *J. Adv. Model. Earth Syst.* **14**, e2021MS002960 (2022).

41. Zeng, J., Iida, Y., Matsunaga, T. & Shirai, T. Surface ocean CO2 concentration and air-sea flux estimate by machine learning with modelled variable trends. *Front. Mar. Sci.* **9**, 989233 (2022).

42. Gloege, L. et al. Quantifying errors in observationally based estimates of ocean carbon sink variability. *Glob. Biogeochem. Cycles* **35**, e2020GB006788 (2021).

43. Hauck, J. et al. Sparse observations induce large biases in estimates of the global ocean CO2 sink: an ocean model subsampling experiment. *Philos. Trans. R. Soc. A: Math. Phys. Eng. Sci.* **381**, 20220063 (2023).

44. Dai, M. et al. Carbon fluxes in the coastal ocean: synthesis, boundary processes, and future trends. *Annu. Rev. Earth Planet. Sci.* **50**, 593–626 (2022).

45. Laruelle, G. G. et al. Continental shelves as a variable but increasing global sink for atmospheric carbon dioxide. *Nat. Commun.* **9**, 454 (2018).

46. Mathis, M. et al. Enhanced CO2 uptake of the coastal ocean is dominated by biological carbon fixation. *Nat. Clim. Chang.* 1–7 https://doi.org/10.1038/s41558-024-01956-w (2024).

47. Regnier, P., Resplandy, L., Najjar, R. G. & Ciais, P. The land-to-ocean loops of the global carbon cycle. *Nature* **603**, 401–410 (2022).

48. Resplandy, L. Coastal sink outpaces open ocean. *Nat. Clim. Chang.* 1–2 https://doi.org/10.1038/s41558-024-01968-6 (2024).

49. Fay, A. R. & McKinley, G. A. Observed regional fluxes to constrain modeled estimates of the ocean carbon sink. *Geophys. Res. Lett.* **48**, e2021GL095325 (2021).

50. Mongwe, N. P., Vichi, M. & Monteiro, P. M. S. The seasonal cycle of pCO_2 and CO_2 fluxes in the Southern Ocean: diagnosing anomalies in CMIP5 Earth system models. *Biogeosciences* **15**, 2851–2872 (2018).

51. Rodgers, K. B. et al. Seasonal variability of the surface ocean carbon cycle: a synthesis. *Glob. Biogeochem. Cycles* **37**, e2023GB007798 (2023).

52. Mayot, N. et al. Climate-driven variability of the Southern Ocean CO2 sink. *Philos. Trans. R. Soc. A: Math. Phys. Eng. Sci.* **381**, 20220055 (2023).

53. Denvil-Sommer, A., Gehlen, M. & Vrac, M. Observation system simulation experiments in the Atlantic Ocean for enhanced surface ocean pCO_2 reconstructions. *Ocean Sci.* **17**, 1011–1030 (2021).

54. Djeutchouang, L. M., Chang, N., Gregor, L., Vichi, M. & Monteiro, P. M. S. The sensitivity of pCO_2 reconstructions to sampling scales across a Southern Ocean sub-domain: a semi-idealized ocean sampling simulation approach. *Biogeosciences* **19**, 4171–4195 (2022).

55. Bourgeois, T., Goris, N., Schwinger, J. & Tjiputra, J. F. Stratification constrains future heat and carbon uptake in the Southern Ocean between 30°S and 55°S. *Nat. Commun.* **13**, 340 (2022).

56. Terhaar, J., Frölicher, T. L. & Joos, F. Southern Ocean anthropogenic carbon sink constrained by sea surface salinity. *Sci. Adv.* **7**, eabd5964 (2021).

57. Terhaar, J., Frölicher, T. L. & Joos, F. Observation-constrained estimates of the global ocean carbon sink from Earth system models. *Biogeosciences* **19**, 4431–4457 (2022).

58. Hauck, J. et al. The Southern ocean carbon cycle 1985–2018: mean, seasonal cycle, trends, and storage. *Glob. Biogeochem. Cycles* **37**, e2023GB007848 (2023).

59. Aumont, O. et al. Riverine-driven interhemispheric transport of carbon. *Glob. Biogeochem. Cycles* **15**, 393–405 (2001).

60. Rödenbeck, C., DeVries, T., Hauck, J., Le Quéré, C. & Keeling, R. F. Data-based estimates of interannual sea–air CO_2 flux variations 1957–2020 and their relation to environmental drivers. *Biogeosciences* **19**, 2627–2652 (2022).

61. Sen, P. K. Estimates of the regression coefficient based on Kendall's Tau. *J. Am. Stat. Assoc.* **63**, 1379–1389 (1968).

62. Theil, H.A. Rank-invariant method of linear and polynomial regression analysis. In: *Henri Theil's Contributions to Economics and Econometrics: Econometric Theory and Methodology* (eds. Raj, B. & Koerts, J.) 345–381 (Springer Netherlands, Dordrecht, 1992). https://doi.org/10.1007/978-94-011-2546-8_20.

63. Lan, X. et al. Atmospheric carbon dioxide dry air mole fractions from the NOAA GML carbon cycle cooperative global air sampling network. https://doi.org/10.15138/wkgj-f215 (2023).

64. Dickson, A. G., Sabine, C. L. & Christian, J. R. Guide to best practices for ocean CO2 measurements. North Pacific Marine Science Organization, 191 (2007).

65. Banzon, V., Smith, T. M., Chin, T. M., Liu, C. & Hankins, W. A long-term record of blended satellite and in situ sea-surface temperature for climate monitoring, modeling and environmental studies. *Earth Syst. Sci. Data* **8**, 165–176 (2016).

66. Weiss, R. F. Carbon dioxide in water and seawater: the solubility of a non-ideal gas. *Mar. Chem.* **2**, 203–215 (1974).

67. Good, S. A., Martin, M. J. & Rayner, N. A. EN4: quality controlled ocean temperature and salinity profiles and monthly objective analyses with uncertainty estimates. *J. Geophys. Res. Oceans* **118**, 6704–6716 (2013).

68. Hersbach, H. et al. ERA5 monthly averaged data on single levels from 1940 to present. https://doi.org/10.24381/cds.f17050d7 (2023).

69. Madec, G. et al. NEMO ocean engine. https://www.earth-prints.org/handle/2122/13309 (2017).

70. Gent, P. R. & Mcwilliams, J. C. Isopycnal mixing in ocean circulation models. *J. Phys. Oceanogr.* **20**, 150–155 (1990).

71. Timmermann, R. et al. On the representation of high latitude processes in the ORCA-LIM global coupled sea ice–ocean model. *Ocean Model.* **8**, 175–201 (2005).

72. Wright, R. M., Le Quéré, C., Buitenhuis, E., Pitois, S. & Gibbons, M. J. Role of jellyfish in the plankton ecosystem revealed using a global ocean biogeochemical model. *Biogeosciences* **18**, 1291–1320 (2021).

73. Buitenhuis, E. T., Le Quéré, C., Bednaršek, N. & Schiebel, R. Large contribution of pteropods to shallow CaCO3 export. *Glob. Biogeochem. Cycles* **33**, 458–468 (2019).

74. Le Quéré, C. et al. Role of zooplankton dynamics for Southern Ocean phytoplankton biomass and global biogeochemical cycles. *Biogeosciences* **13**, 4111–4133 (2016).

75. Bakker, D. C. E. et al. Surface ocean CO2 atlas database version 2023 (SOCATv2023) (NCEI Accession 0278913). https://www.ncei.noaa.gov/access/metadata/landing-page/bin/iso?id=gov.noaa.nodc:0278913 (2023).

Acknowledgements

Author contributions

N.M. and C.L.Q. conceived the study. C.L.Q., E.T.B. and R.M.W. designed and performed the NEMO-PlankTOM12.1 model simulations. D.C.E.B. supervised the collation and use of the SOCAT database. J.H. supervised the use and interpretation of the global carbon budget database. E.T.B. developed the theory of the hybrid approach. N.M. carried out the implementation of the hybrid approach and performed all complementary analysis. N.M. wrote the manuscript with input from all authors. C.L.Q. supervised the study.

Competing interests

The authors declare no competing interests.

Additional information

Supplementary information The online version contains supplementary material available at https://doi.org/10.1038/s41467-024-52641-7.

Correspondence and requests for materials should be addressed to Nicolas Mayot.

Peer review information *Nature Communications* thanks the anonymous reviewers for their contribution to the peer review of this work. A peer review file is available.

Reprints and permissions information is available at http://www.nature.com/reprints

Publisher's note Springer Nature remains neutral with regard to jurisdictional claims in published maps and institutional affiliations.